Article

JOURNAL OF COMPOSITE MATERIALS

Journal of Composite Materials
0(0) 1–10

DOI: 10.1177/0021998317751284
journals.sagepub.com/home/jcm
SAGE

Influence of axial compressive loads on buckling and free vibration response of surface-modified fly ash cenosphere/epoxy syntactic foams

Sunil Waddar, P Jeyaraj and Mrityunjay Doddamani

Abstract

This work deals with experimental buckling and free vibration behavior of silane-treated cenosphere/epoxy syntactic foams subjected to axial compression. Critical buckling loads are computed from compressive load–deflection plots deduced using universal testing machine. Further, compressive loads are applied in the fixed intervals until critical loading point on different set of samples having similar filler loadings to estimate natural frequency associated with the first three transverse bending modes. Increasing filler content increases critical buckling load and natural frequency of syntactic foam composites. Increasing axial compressive load reduce structural stiffness of all the samples under investigation. Syntactic foams registered higher stiffness compared to neat epoxy for all the test loads. Similar observations are noted in case of untreated cenosphere/epoxy foam composites. Silane-modified cenosphere embedded in epoxy matrix registered superior performance (rise in critical buckling load and natural frequencies to the tune of 23.75% and 11.46%, respectively) as compared to untreated ones. Experimental results are compared with the analytical solutions that are derived based on Euler–Bernoulli hypothesis and results are found to be in good agreement. Finally, property map of buckling load as a function of density is presented by extracting values from the available literature.

Keywords

Buckling, free vibration, fly ash, syntactic foam

Introduction

Dispersion of hollow fly ash cenospheres in matrix resin results in closed cell structured foams, called as syntactic foams. Incorporation of fly ash cenospheres in polymers[1–5] and elastomers leads to reduction in warpage, shrinkage, and weight in addition to resistance to moisture absorption and better surface finish.[6] Thin-walled structural members under axial compression are subjected to buckling mode of failure. Axial compression load develops pre-stress in the structure which in turn alters structural stiffness and hence changes dynamic characteristics of the structure. Owing to their higher specific properties, syntactic foam composites are widely used in automotive, marine, and aviation sectors.[7] This fact necessitates buckling and dynamic behavior investigation of such lightweight composite system.

Previous studies on syntactic foams have reported that the wall thickness, volume fraction, and functional grading of hollow particles can be used effectively to tailor the mechanical properties.[8–15] Fly ash cenospheres have numerous defects on its surface which may compromise mechanical properties.[2] Failure mechanisms in the syntactic foam composites are governed by the interface topology. Enhancement in overall mechanical properties strongly depends on load transfer mechanism which in turn is governed by interfacial bonding between the constituents.[16,17] Gu et al.[18] investigated dynamic mechanical analysis and impact toughness of surface-modified cenospheres/epoxy composites and observed that the composite

Department of Mechanical Engineering, National Institute of Technology Karnataka, India

Corresponding author:
P Jeyaraj, Department of Mechanical Engineering, National Institute of Technology Karnataka, Surathkal, India.
Email: pjeyaemkm@gmail.com

filled with surface-modified fly ash cenospheres have wider glass transition temperature region and higher loss factor and impact toughness. Wu et al.[19] investigated dynamic mechanical analysis of polyurethane-modified epoxy resin filled with silane-treated fly ash particulates and observed higher damping compared to untreated samples and have broad glass transitions temperature peaks. Sroka et al.[20] observed enhancement of tensile strength, Young's modulus, fracture toughness, and thermal conductivity of silanized fly ash particles embedded in epoxy resin. Enhancement of damping and decomposition temperature of epoxy resin with increase in volume fraction of silane-treated fly ash was observed by Gu et al.[21] Gu et al.[22] investigated effect of porosity on damping properties of epoxy composites filled with silane-treated fly ash cenospheres. They observed that damping capacity of the composites increased with increase in porosity.

Most of the studies carried out on thermosetting syntactic foam composites are related to prediction of its mechanical properties and failure mechanism under tension, compression, flexural, and impact loadings.[13,23–26] However, experimental studies on buckling characteristics of syntactic foam composites are not available to the best of author's knowledge. Shams et al.[27] investigated non-linear buckling analysis of spherical shell embedded in an elastic medium under uniaxial compressive load. Numerical investigations revealed that failure of syntactic foam is not governed by the microballoon buckling rather it is a function of shearing force acting on microballoon surface. Tuttle et al.[28] investigated buckling behavior of graphite epoxy laminates subjected to bidirectional loading. They observed that the buckling load increases with the load ratio (applied transverse load to predicted buckling load). Buckling instabilities with axial stresses is investigated by Matsunaga[29,30] and observed a good agreement between Themoshenko beam theory and experimental results. Variations of buckling stresses and loads obtained from numerical model are compared with experimental results for pre and post-buckling behavior of glass/epoxy composites subjected to axial compression load are presented in SudhirSastry et al.[31] Yang et al.[32] investigated buckling and post-buckling of functionally graded multilayer graphene platelet reinforced composite beams based on shear deformation theory. Their studies reveal higher resistance to buckling with addition of graphene platelet nanofillers. Rajesh and Pitchaimani[33] investigated buckling and free vibration behavior of natural fiber fabric composite beam under axial compression. Their Weaving pattern of the fabric has significant influence on buckling strength as noted by them. They also observed that natural frequencies of the beam reduce with increase in axial compressive load. Turvey and Zhang[34] experimentally investigated buckling of glass fiber reinforced composites subjected to uniaxial compression and compared the results with two-dimensional finite element method. Their observations are in good agreement at initial load, deviating later due geometric nonlinearities because of pre-stress effects.

Lateral vibrations of thin-walled structures are of practical interest. Amba-Rao[35] investigated fundamental frequencies in lateral vibration mode for straight bars under compressive loads for various fractions (less than one) of the Euler load for various boundary conditions. Later Galef[36] presented an approximate formulation relating fundamental natural frequencies of compressed and uncompressed beam with applied compressive and Euler buckling load. Shaker's[37] investigations resulted in expressions for mode shape and characteristics equations for various boundary conditions. The effect of preload on natural frequencies and mode shape are represented graphically. Bokaian[38] presented analytical solutions for variation of natural frequencies of an isotropic beam subjected to axial compression loads under various boundary conditions and found that Galef's expression is not valid for pinned-free and free-free beams.

Present work deals with experimental investigations of buckling and free vibration response of silane-treated cenosphere/epoxy syntactic foams. These low-cost lightweight materials have potential to replace conventional materials in various applications such as automobiles, marine, and aerospace. Treated and untreated cenospheres are varied by 20, 40 and 60 vol% in epoxy resin. Cenospheres are treated with silane to strengthen interfacial bonding between the constituents. Cenospheres are mixed manually with epoxy resin and gravity casting route is adopted for processing of all the samples. Neat epoxy samples are also casted for comparative studies. Experimental buckling loads are estimated using Double Tangent Method (DTM), Modified Budiansky Criteria (MBC) and compared with analytical formulations based on Euler–Bernoulli. Finally, fundamental frequency is estimated for first three transverse free vibration modes with varying axial load and compared with analytical results. Buckling and vibration investigations of syntactic foams are very crucial from the structural stability point of view and hence presented herewith.

Materials and methods

Constituent materials

Epoxy resin (LAPOX L-12) as matrix and room temperature curing agent polyamine (K-6) as hardener (Atul Ltd, Gujarat, India) are the constituent materials used in this work. Cenosphere of CIL 150 grade

procured from Cenosphere India Pvt. Ltd, Kolkata, West Bengal, India, is used as filler. 3-Aminopropyl tri ethoxy silane (APTS), procured from Sigma Aldrich (USA), is utilized for surface treatment of cenospheres.

Silane treatment of cenospheres

Water/ethanol mixture in the weight proportion of 20:80 is prepared and maintained at 80°C. In this 100 ml solution, 50 g of cenospheres are mixed. Solution is continuously stirred for 30 min at 80°C in a microwave reactor (Enerzi Microwave Systems, Bangalore) after adding APTS 2% by volume. Treated cenospheres are extracted after resultant product is filtered and washed at least three times using a mixture of water/ethanol post-drying in an oven. Fourier transform infrared (FTIR) spectroscopy is conducted on cenospheres to confirm the silane coating.

FTIR and particle size analysis

FTIR spectroscopy of cenospheres is carried out on JASCO 4200 (Japan) with automated total reflection mode using wavenumber in the range of 4000 to 650 cm^{-1}. X-ray diffractograms are obtained for 2θ values using DX GE-2P, Japan, having nickel filter material with scanning speed of 2°/min and Cu Kα ($\lambda = 1.514$ A°) radiation. Particle size and shape analysis is carried out on Sympatec (Pennington, NJ) QICPIC high-speed analysis system.

Syntactic foam preparation

Silane-treated fly ash cenospheres with 20, 40, and 60 vol% are mixed in epoxy resin. Treated cenospheres and epoxy resin are weighed in a predetermined quantity and stirred slowly until homogenous slurry is formed to be decanted into aluminum mold. Polymerization process is initiated by adding 10 wt% of K6 hardener into the slurry before pouring it into the mold. Silicone releasing agent is applied to the mold for easy removal of cast slabs. The castings are allowed to cure for 24 h at room temperature and trimmed using diamond saw to the dimensions of $310 \times 12.5 \times 4$ mm. All samples are coded as per nomenclature EXX, where letter 'E' denote neat epoxy resin, 'XX' represents cenosphere volume fraction. Neat epoxy sample is also prepared for comparison.

Density test

Experimental densities of treated fly ash cenosphere/epoxy syntactic foams are estimated as per ASTM D792-13. Five samples of each composition are tested and the average values and standard deviations are reported (Table 1). The theoretical densities of syntactic foams are calculated using rule of mixtures. The air entrapped during manual mixing of cenospheres in epoxy is referred as void content. Void content (Φ_v) in the syntactic foam is computed by accounting for the relative difference between the theoretical (ρ^{th}) and experimentally measured ($\rho^{\exp}$) density[9]

$$\Phi_v = \frac{\rho^{th} - \rho^{\exp}}{\rho^{th}} \quad (1)$$

Buckling test

Buckling test of silane-treated fly ash cenosphere/epoxy syntactic foams in clamped–clamped condition subjected to axial compression is carried out on Universal Testing Machine (H75KS, Tinius Olsen make, UK) having a load cell capacity of 50 kN. Cross-head displacement rate is maintained at the rate of 0.2 mm/min. Five specimens having unclamped length of 210 mm, width 12.5 mm, and thickness 4 mm are tested and average values are reported. As there is no specific standard available for the buckling test, specimen with above dimension which follows Euler–Bernoulli hypothesis[39] is considered. Figure 1 presents the experimental setup of the buckling and free vibration test under axial compression. For all the samples tested, the end shortening limit is set at 0.75 mm to explore the possibility of behavioral changes, if any, in post-buckling regime. Critical buckling load (P_{cr}) is

Table 1. Theoretical and experimental densities of pure epoxy and syntactic foams.

Sample coding	Theoretical density (kg/m^3)	Experimental density (kg/m^3)	Void content (%)	% Reduction in density
E0	1189.54	1189.54 ± 1.05	~	~
E20	1151.63	1122.05 ± 3.69	2.57	5.67
E40	1113.72	1062.10 ± 3.70	4.63	10.71
E60	1075.82	1015.75 ± 3.71	5.58	14.61

determined graphically using DTM and MBC techniques (Figure 2) based on experimentally acquired load–deflection data.[28,40] DTM is a two-tangent method wherein tangents are drawn in pre- and post-buckling regimes. Intersection point of two tangents determines the P_{cr} as presented in Figure 2(a), whereas load value corresponding to a bisector at the intersection points of both the tangents determines P_{cr} in Budiansky criteria (Figure 2(b)). DTM and MBC techniques are used to estimate upper and lower bounds of P_{cr} which helps in carefully designing structures.

Free vibration test

Experimental modal analysis is used to predict first three natural frequencies corresponding to first three bending modes of samples subjected to compressive load under clamped–clamped condition. Figure 1 shows schematic representation of experimental setup utilized. Roving hammer method is used to excite the samples and the vibration signals are recorded by a uniaxial accelerometer. Kitsler make impulse hammer (9722A2000, sensitivity of 10 mV/N) and light weight accelerometer (8778A500, sensitivity of 10 mV/g) with operating range of ± 500 g are used. Accelerometer is mounted on the specimen using bee's wax. The response signals are collected by DEWESoft software wherein time domain signals are converted into frequency domain using Fast Fourier Transform algorithm to report natural frequency and mode shapes. The experimental modal analysis is carried out at every increment load of 50 N. The application of compressive load is paused for 2 min to perform modal analysis.

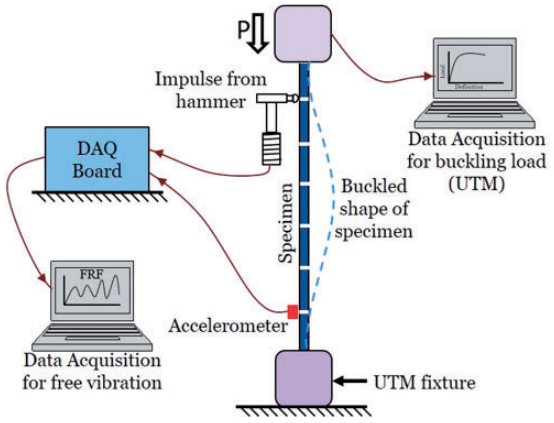

Figure 1. Schematic representation of experimental setup used for buckling and free vibration test under axial compression loads. P is axial compressive load.

Determination of Young's modulus of syntactic foams using Bardella–Genna model (theoretical approach)

Modulus estimated by Bardella–Genna model[41] is used in analytical and FEA simulations. Homogenous scheme is used in this model to predict bulk and shear modulus and is given by[41]

$$K_{bulk} = K_m \frac{\delta(1+\Phi_\gamma) + \kappa(1+\Phi)\gamma}{\delta(1-\Phi) + \kappa(\gamma+\Phi)} \tag{2}$$

where $\gamma = \frac{4G_m}{3K_m}$, $\delta = \frac{4G_i}{3K_m}(1-\eta^3)$, $\kappa = \frac{4G_i}{3K_i} + \eta^3$, $\eta = 0.9$, K_{bulk}, and G are bulk and shear moduli; subscripts m and i represent matrix and inclusions, respectively, Φ designates filler volume fraction. Young's modulus and Poisson's ratio of the cenosphere are 158 GPa and 0.19, respectively.[3] The constants listed in literature[1,3] predicted very high values of elastic modulus of foams, thereby curve fitting method is adopted to deduce Young's modulus and radius ratio (η) of cenosphere and is found to be 74 GPa and 0.85, respectively. The modulus of matrix material is obtained using[42]

$$E = \left(\frac{\omega_j}{\beta_j^2}\right)^2 \left(\frac{\rho^{\exp} A L^4}{I}\right) \tag{3}$$

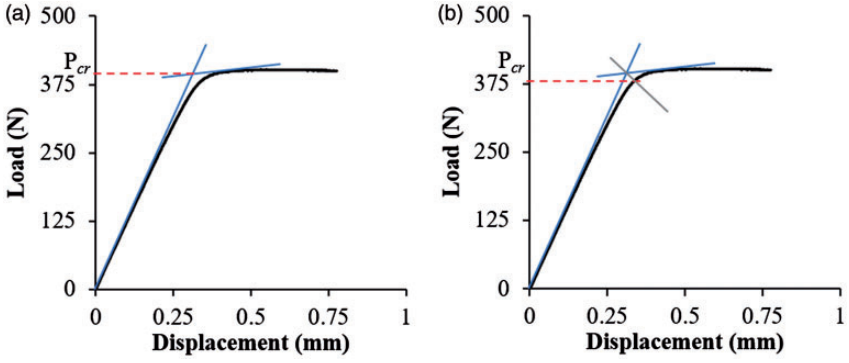

Figure 2. Representative load–deflection plots for determining critical buckling load: (a) DTM and (b) MBC for E40 sample.

where ω_j is the angular natural frequency ($\omega = 2\pi f$, where f is natural frequency obtained from free vibration test), β is a constant (4.73 for first mode, for clamped–clamped boundary condition), E is Young's modulus, and I is the moment of inertia. $\rho^{\exp}$ is the experimental density of syntactic foams and A is the cross-sectional area. Poisson's ratio of epoxy resin is 0.35.[43,44] Density and Poisson's ratio of the syntactic foams is estimated using rule of mixtures. Modulus is given by

$$E = \frac{9KG}{3K + G} \tag{4}$$

Theoretical formulation

Fly ash cenospheres are spherical in shape. Thereby, cenosphere/epoxy composite foam can be modeled as isotropic material. Further, syntactic foam is assumed to behave as linearly elastic. Neglecting shear deformation and rotary inertia effects, beam differential equation of motion subjected to axial compression is given by[38]

$$EI\left(\frac{\partial^4 y(x)}{\partial x^4}\right) + P\left(\frac{\partial^2 y(x)}{\partial x^2}\right) - \rho A\left(\frac{\partial^2 y}{\partial t^2}\right) = 0 \tag{5}$$

where $y = y(x, t)$ is the transverse displacement, E is the elastic modulus, I is the moment of inertia, A is the cross-sectional area, and ρ is the density of material.

If $y(x, t) = Y(x)\cos\omega t$ for the normal mode oscillation of the beam, then equation (5) becomes

$$EI\left(\frac{d^4 Y(x)}{dx^4}\right) + P\left(\frac{d^2 Y(x)}{dx^2}\right) - \rho A\omega^2 Y(x) = 0 \tag{6}$$

where ω is the circular natural frequency and Y(x) is the modal displacement. Considering dimensionless beam co-ordinate $\zeta = \frac{x}{l}$ ($0 \le \zeta \le l$), solution to equation (6) can be written as

$$\begin{aligned} Y(x) = Y(l\zeta) = {} & C_1 \sinh Q\zeta + C_2 \cos Q\zeta \\ & + C_3 \sin R\zeta + C_4 \cos R\zeta \end{aligned} \tag{7}$$

where C_1, C_2, C_3, and C_4, are constant coefficients, Q and R are defined as

$$Q = l\sqrt{\left\{-\left(\frac{P}{2EI}\right) + \sqrt{\left[\left(\frac{P}{2EI}\right)^2 + \left(\frac{\rho A}{EI}\right)\omega^2\right]}\right\}}$$

$$R = l\sqrt{\left\{\left(\frac{P}{2EI}\right) + \sqrt{\left[\left(\frac{P}{2EI}\right)^2 + \left(\frac{\rho A}{EI}\right)\omega^2\right]}\right\}}$$

$$Q = \sqrt{\left(-U + \sqrt{U^2 + \Omega^2}\right)}$$

$$R = \sqrt{\left(U + \sqrt{U^2 + \Omega^2}\right)}$$

where $U = \frac{Pl^2}{2EI}$ is the relative axial force, $\Omega = \frac{\omega l^2}{\alpha}$ is the relative natural frequency, $\alpha = \sqrt{\frac{EI}{\rho A}}$ is the constant parameter. Differentiating equation (7) we get

$$\begin{aligned} \frac{dY}{dx} = {} & QC_1 \cosh Q\xi + QC_2 \sinh Q\xi \\ & + RC_3 \cos R\xi - NC_4 \sin R\xi \end{aligned} \tag{8}$$

The boundary conditions for clamped–clamped case are

$$Y(x) = 0; \quad \frac{dY(0)}{dx} = 0; \quad Y(l) = 0; \quad \frac{dY(l)}{dx} = 0 \tag{9}$$

Substituting the boundary conditions (equation (9)) in equations (7) and (8) results in non-trivial solution. For the non-trivial solution taking detriment of coefficient as zero we get

$$\begin{vmatrix} 0 & 1 & 0 & 1 \\ Q & 0 & R & 0 \\ \sinh Q & \cosh Q & \sin R & \cos R \\ Q\cosh Q & Q\sinh Q & R\cos R & -R\sin R \end{vmatrix} = 0$$

$$\left(Q^2 - R^2\right)\sin R \sinh Q + 2QR(1 - \cos R \cosh Q) = 0 \tag{10}$$

Substituting Q and R in terms of U and Ω in equation (10)

$$\begin{aligned} & \Omega - U\sin\sqrt{\left(U + \sqrt{U^2 + \Omega^2}\right)}\sinh\sqrt{\left(-U + \sqrt{U^2 + \Omega^2}\right)} \\ & - \Omega\cos\sqrt{\left(U + \sqrt{U^2 + \Omega^2}\right)}\cosh\sqrt{\left(-U + \sqrt{U^2 + \Omega^2}\right)} = 0 \end{aligned} \tag{11}$$

Equation (11) is the characteristics equation for variation of natural frequency as a function of compressive load. This equation is solved numerically with MATLAB code to obtain the frequency–compressive load plot.

Results and discussion

Material processing

FTIR spectroscopy results for silane-treated and untreated cenospheres are presented in Figure 3(a). The spectrum confirms the presence of silane layer on as received cenospheres. The characteristics peak of 3-aminopropyl tri ethoxy silane has a band lying in around 2900 cm^{-1} representing an absorbing peak of C–H bond, which belongs to CH_3. In the FTIR, the peak absorbed for fly ash cenospheres with surface modification is seen at 2929 cm^{-1}. This peak is absent in the spectrum for untreated fly ash cenospheres suggesting peak of 3-aminopropyl tri ethoxy silane.[18] Figure 3(b) shows particle size analysis, the × 50 weighted average median of untreated cenosphere and treated cenospheres is 55.08 and 48.24, respectively. It can be observed from Figure 3(b) that the peak for treated cenosphere shift towards right-hand side and is broader indicating increase in particle size compared to untreated cenospheres. Density of untreated and treated cenospheres is found to be 920 and 1000 kg/m^3. Surface modification results in 8.69% rise in density which is still lower than the epoxy resin indicating possible avenues of weight reduction.

Density

Density of the syntactic foam is computed to analyse weight saving potential, matrix porosity, and particle breakage during processing, if any. Table 1 presents theoretical and experimental densities of pure epoxy and syntactic foams. Density of cenosphere/epoxy syntactic foams decreases in the range of 5.67–14.61% with increasing filler content as compared to neat epoxy. Decrease in density is attributed to increase in number of hollow microballoons embedded into epoxy matrix. Void content increases in a narrow range (≤5.58%) with higher cenosphere loadings as observed from Table 1. Lower void contents signify consistency in processing route and good quality of the samples.

Buckling test

Schematic diagram of the experimental setup used to perform buckling test is presented in Figure 1. For all the tested samples, the maximum deflection under axial compressive load is observed to appear in the middle of the sample lengthwise (Figure 1). Buckling load shows increasing trend as a function of filler content (Figure 4 and Table 2). Higher loading of the silane-treated cenospheres in matrix enhances modulus and hence overall stiffness of the syntactic foams. Further, it also depends on relative difference between constituent moduli. Cenosphere modulus is almost 19 times higher than that of epoxy matrix resulting in higher P_{cr} for syntactic foams. P_{cr} for neat epoxy is 237.67 N. Rise in buckling

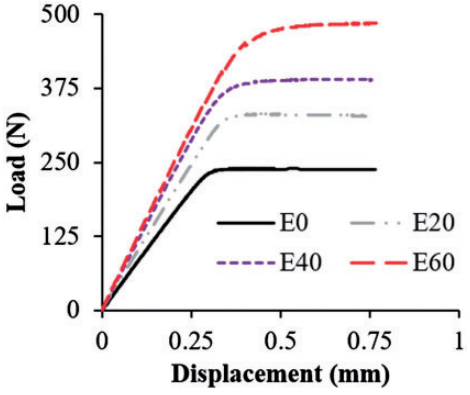

Figure 4. A representative set of graphs showing experimental buckling behavior of neat epoxy and their syntactic foams.

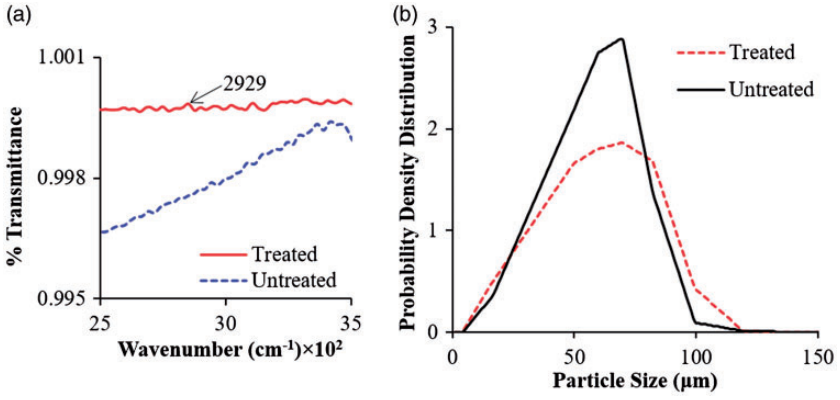

Figure 3. FTIR spectroscopy and particle size analysis of untreated and treated cenospheres.

Table 2. Experimental and theoretical critical buckling load for pure epoxy and syntactic foams.

Sample coding	Experimental P_{cr} (N)		Theoretical P_{cr} (N)
	DTM	MBC	
E0	237.67 ± 11.02	231.83 ± 12.51	233.88
E20	315.50 ± 12.78	306.67 ± 12.52	292.41
E40	393.85 ± 16.37	383.83 ± 17.29	366.38
E60	479.33 ± 17.76	470.67 ± 16.16	460.37

Table 3. Comparison of Young's modulus values obtained from frequency data and Bardella–Genna model for pure epoxy and syntactic foams.

Sample coding	Young's modulus (MPa)		
	Frequency data (equation (3))	Bardella–Genna model	% Difference
E0	3917.81 ± 105.79	3917.81	–
E20	5088.47 ± 160.89	4898.40	3.74
E40	6397.46 ± 128.92	6137.50	4.06
E60	7422.55 ± 75.73	7712.00	−3.89

load is in the range of 32.75–101.67% and 32.28–103.02% with increasing filler volume using DTM and MBC approaches compared to their respective values for E0.

Theoretical critical buckling load for clamped–clamped beam calculated based on Euler–Bernoulli assumption[39] is $P_{cr} = \frac{4\pi^2 EI}{L^2}$ where E is Young's modulus obtained from Bardella–Genna model (Table 3), I is the moment of inertia, L is the unclamped length of the beam. Table 3 represents Young's modulus obtained using equation (3) and Bardella–Genna model. The modulus values increase in the range of 29.88% to 89.45% for increase in filler content from 20% to 60%. Natural frequencies of syntactic foams show an increasing trend with increasing in filler content. The increase in natural frequency of syntactic foams can be attributed to increase in overall stiffness of the composite due to the addition of stiffer cenospheres and also enhancement of stiffness due to proper interfacial bonding of particles and matrix, as a result of silane treatment of cenospheres. Further, increase in mean particle diameter also augments the stiffness values.

Natural frequencies variation under axial compressive loads

Experimentally obtained natural frequencies corresponding to first three bending mode shapes are compared with the analytical solution (equation (11)). Frequency response functions (FRFs) are used to find natural frequencies corresponding to first three bending mode shapes using DEWESoft software. A typical FRF response associated with E20 syntactic foam is presented in Figure 5.

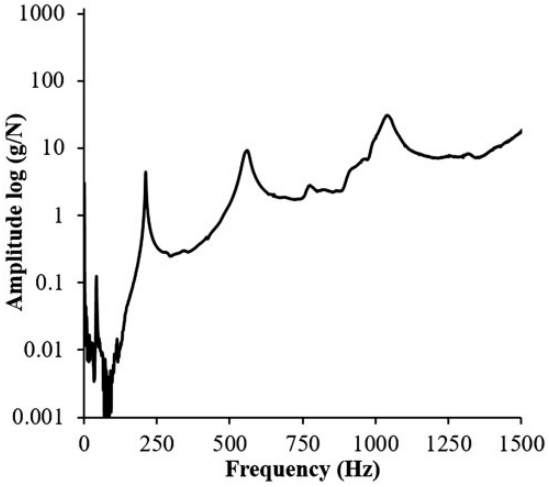

Figure 5. Frequency response function of E20 sample.

With increase in compressive load decrease in natural frequency is observed for all samples tested. Experimentally, the first natural frequency reaches minimum value at onsite of buckling and increases rapidly in post-buckling region due to geometric stiffness gain resulting from beam deflection. Similar trend is observed in previous studies[33] on isotropic/composite beam and columns. Theoretically, first natural frequency becomes zero when the beam is subjected to axial compressive load which is equivalent to critical buckling load (Figure 6). The first natural frequency decreases steadily till the compressive load approaches critical buckling load. First natural frequency drops suddenly due to loss of structural stiffness when the compressive load is very closer to critical buckling load.

Comparison with untreated cenosphere/epoxy syntactic foams

Variation of critical buckling load and fundamental natural frequency with respect to cenosphere loading for treated and untreated syntactic foam beams is shown in Figure 7. It can be observed that the buckling load and natural frequencies of silane-treated cenosphere/epoxy foams are higher than that of the untreated ones. This enhancement in buckling load and natural frequencies can be attributed to strong interfacial bonding between the particles and matrix material, which in turn increases structural stiffness of the samples. The silane-treated cenosphere/epoxy

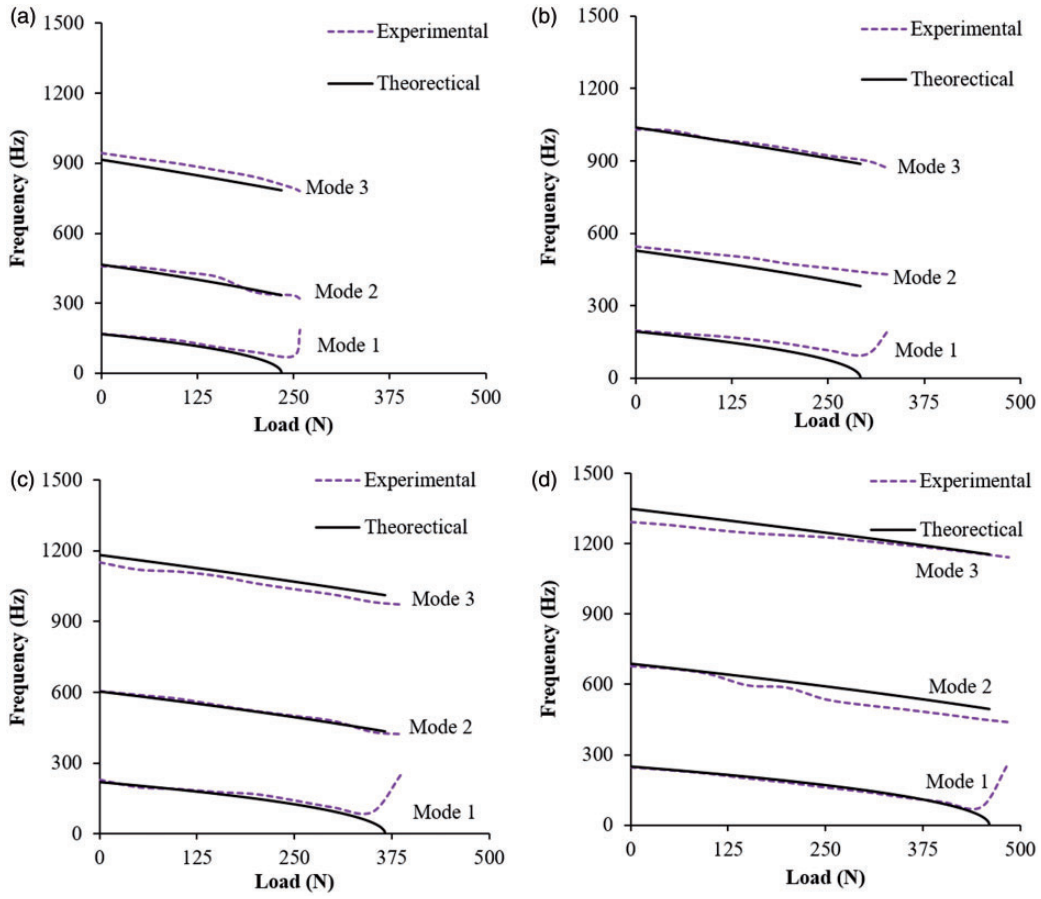

Figure 6. Influence of compressive load on natural frequency of (a) E0 (b) E20 (c) E40 (d) E60 samples.

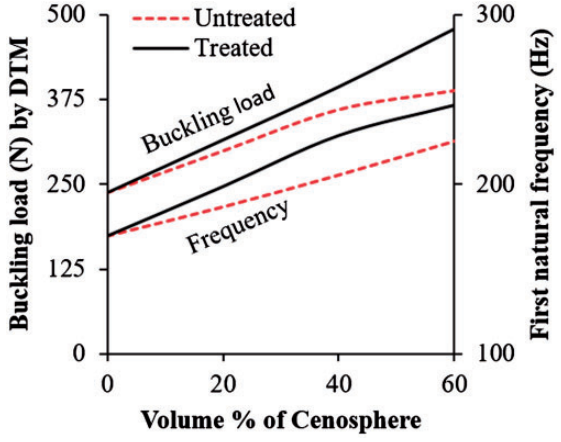

Figure 7. Comparison of buckling load using DTM and first natural frequency of untreated and treated cenosphere syntactic foams.[44]

syntactic foams show enhancement of buckling load up to 23.75% and natural frequency up to 11.46% as compared to untreated cenosphere/epoxy syntactic foams.

Lower density of syntactic foams is the most promising feature that enables their application for lightweight structures. Variation of critical buckling load with density of composites available in the literature is analyzed in the present work and is plotted in Figure 8. Data are extracted for untreated cenosphere/epoxy syntactic foams and natural fiber reinforced thermosetting composites which find applications in low and medium load structural components. Figure 8 shows that appropriate choice of constituent materials and concentrations can help in designing structural components subjected to axial compressive loads, where buckling mode failure is predominant. It can be observed that natural fiber composite is more susceptible for buckling failure than syntactic foam composites. Density of syntactic foams is lower than natural fiber composites implying weight reduction. Thin and lightweight structural components are desired to have higher buckling loads for lower densities, where syntactic foams can provide advantage over their specific properties comparable to several composites having absolute properties.

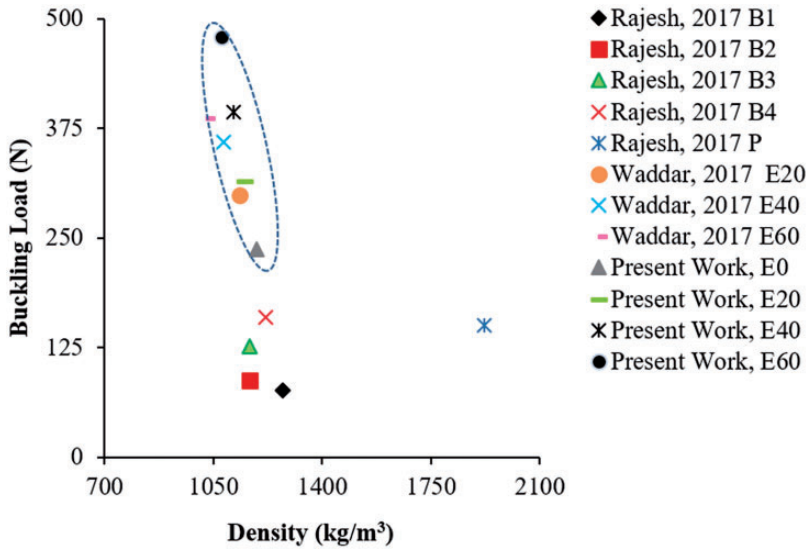

Figure 8. Buckling load plotted against density from available studies.[33,44,45]

Conclusions

Buckling and free vibrations characteristics of treated fly ash cenosphere/epoxy syntactic foams are investigated experimentally and compared with analytical results. The buckling load and natural frequencies increase with increase in cenosphere volume fraction. With increase in compressive load, decrease in natural frequency is observed for all samples tested. Experimentally, the first natural frequency reaches minimum value at onsite of buckling and increases rapidly in post-buckling region. The buckling load and natural frequencies of silane-treated cenosphere/epoxy foams are higher than that of the untreated ones. Property map of buckling load as a function of density is presented by extracting values from the available literature. Density of syntactic foams is lower than other composites considered resulting in weight reduction leading to higher specific properties.

Acknowledgements

The authors thank the Mechanical Engineering Department at the National Institute of Technology Karnataka for providing facilities and support.

Declaration of Conflicting Interests

The author(s) declared no potential conflicts of interest with respect to the research, authorship, and/or publication of this article.

Funding

The author(s) received no financial support for the research, authorship, and/or publication of this article.

References

1. Bharath Kumar BR, Doddamani M, Zeltmann SE, et al. Processing of cenosphere/HDPE syntactic foams using an industrial scale polymer injection molding machine. *Mater Des* 2016; 92: 414–423.
2. Bharath Kumar BR, Doddamani M, Zeltmann SE, et al. Effect of particle surface treatment and blending method on flexural properties of injection-molded cenosphere/HDPE syntactic foams. *J Mater Sci* 2016; 51: 3793–3805.
3. Bharath Kumar BR, Zeltmann SE, Doddamani M, et al. Effect of cenosphere surface treatment and blending method on the tensile properties of thermoplastic matrix syntactic foams. *J Appl Polym Sci* 2016; 133. DOI: 10.1002/app.43881.
4. Bharath Kumar BR, Singh AK, Doddamani M, et al. Quasi-static and high strain rate compressive response of injection-molded cenosphere/HDPE syntactic foam. *JOM* 2016; 68: 1861–1871.
5. Zeltmann SE, Prakash KA, Doddamani M, et al. Prediction of modulus at various strain rates from dynamic mechanical analysis data for polymer matrix composites. *Compos B Eng* 2017; 120: 27–34.
6. Figovsky O, Beilin D, Blank N, et al. Development of polymer concrete with polybutadiene matrix. *Cem Concr Compos* 1996; 18: 437–444.
7. Gupta N, Zeltmann SE, Shunmugasamy VC, et al. Applications of polymer matrix syntactic foams. *JOM* 2014; 66: 245–254.
8. Tagliavia G, Porfiri M and Gupta N. Analysis of hollow inclusion–matrix debonding in particulate composites. *Int J Solids Struct* 2010; 47: 2164–2177.
9. Tagliavia G, Porfiri M and Gupta N. Analysis of flexural properties of hollow-particle filled composites. *Compos B Eng* 2010; 41: 86–93.

10. Gupta N. A functionally graded syntactic foam material for high energy absorption under compression. *Mater Lett* 2007; 61: 979–982.
11. Jayavardhan ML, Bharath Kumar BR, Doddamani M, et al. Development of glass microballoon/HDPE syntactic foams by compression molding. *Compos B Eng* 2017; 130: 119–131.
12. Manakari V, Parande G, Doddamani M, et al. Dry sliding wear of epoxy/cenosphere syntactic foams. *Tribol Int* 2015; 92: 425–438.
13. Labella M, Zeltmann SE, Shunmugasamy VC, et al. Mechanical and thermal properties of fly ash/vinyl ester syntactic foams. *Fuel* 2014; 121: 240–249.
14. Doddamani M, Kishore, Shunmugasamy VC, et al. Compressive and flexural properties of functionally graded fly ash cenosphere–epoxy resin syntactic foams. *Polym Compos* 2015; 36: 685–693.
15. Gupta N, Woldesenbet E and Mensah P. Compression properties of syntactic foams: effect of cenosphere radius ratio and specimen aspect ratio. *Compos A Appl Sci Manuf* 2004; 35: 103–111.
16. Wang W, Li Q, Wang B, et al. Synthesis of fly ash cenosphere/polyaniline and mullite/polyaniline core–shell composites. *Mater Chem Phys* 2012; 135: 1077–1083.
17. Guhanathan S, Devi MS and Murugesan V. Effect of coupling agents on the mechanical properties of fly ash/polyester particulate composites. *J Appl Polym Sci* 2001; 82: 1755–1760.
18. Gu J, Wu G and Zhao X. Effect of surface-modification on the dynamic behaviors of fly ash cenospheres filled epoxy composites. *Polym Compos* 2009; 30: 232–238.
19. Wu G, Gu J and Zhao X. Preparation and dynamic mechanical properties of polyurethane-modified epoxy composites filled with functionalized fly ash particulates. *J Appl Polym Sci* 2007; 105: 1118–1126.
20. Sroka J, Rybak A, Sekula R, et al. An investigation into the influence of filler silanization conditions on mechanical and thermal parameters of epoxy resin-fly ash composites. *J Polym Environ* 2016; 24: 298–308.
21. Gu J, Wu G and Zhang Q. Preparation and damping properties of fly ash filled epoxy composites. *Mater Sci Eng A* 2007; 452: 614–648.
22. Gu J, Wu G and Zhang Q. Effect of porosity on the damping properties of modified epoxy composites filled with fly ash. *Scr Mater* 2007; 57: 529–532.
23. Wouterson EM, Boey FYC, Hu X, et al. Specific properties and fracture toughness of syntactic foam: effect of foam microstructures. *Compos Sci Technol* 2005; 65: 1840–1850.
24. Colloca M, Gupta N and Porfiri M. Tensile properties of carbon nanofiber reinforced multiscale syntactic foams. *Compos B Eng* 2013; 44: 584–591.
25. Gupta N, Ye R and Porfiri M. Comparison of tensile and compressive characteristics of vinyl ester/glass microballoon syntactic foams. *Compos B Eng* 2010; 41: 236–245.
26. Nguyen NQ and Gupta N. Analyzing the effect of fiber reinforcement on properties of syntactic foams. *Mater Sci Eng A* 2010; 527: 6422–6428.
27. Shams A, Aureli M and Porfiri M. Nonlinear buckling of a spherical shell embedded in an elastic medium with imperfect interface. *Int J Solids Struct* 2013; 50: 2310–2327.
28. Tuttle M, Singhatanadgid P and Hinds G. Buckling of composite panels subjected to biaxial loading. *Exp Mech* 1999; 39: 191–201.
29. Matsunaga H. Free vibration and stability of thin elastic beams subjected to axial forces. *J Sound Vib* 1996; 191: 917–933.
30. Matsunaga H. Buckling instabilities of thick elastic beams subjected to axial stresses. *Comput Struct* 1996; 59: 859–868.
31. SudhirSastry YB, Budarapu PR, Madhavi N, et al. Buckling analysis of thin wall stiffened composite panels. *Comput Mater Sci* 2015; 96: 459–471.
32. Yang J, Wu H and Kitipornchai S. Buckling and post-buckling of functionally graded multilayer graphene platelet-reinforced composite beams. *Compos Struct* 2017; 161: 111–118.
33. Rajesh M and Pitchaimani J. Experimental investigation on buckling and free vibration behavior of woven natural fiber fabric composite under axial compression. *Compos Struct* 2017; 163: 302–311.
34. Turvey GJ and Zhang Y. A computational and experimental analysis of the buckling, postbuckling and initial failure of pultruded GRP columns. *Comput Struct* 2006; 84: 1527–1537.
35. Amba-Rao CL. Effect of end conditions on the lateral frequencies of uniform straight columns. *J Acoust Soc Am* 1967; 42: 900–1.
36. Galef AE. Bending frequencies of compressed beams. *J Acoust Soc Am* 1968; 44: 643.
37. Shaker FJ. *Effect of axial load on mode shapes and frequencies of beams*. Washington, USA: National Aeronautics and Space Administration. NASA Technical Note (TN D-8109), 1975.
38. Bokaian A. Natural frequencies of beams under compressive axial loads. *J Sound Vib* 1988; 126: 49–65.
39. Gere JM and Timoshenko SP. *Mechanics of materials*, 2nd ed. New Delhi: CBS Publishers & Distributors Pvt. Ltd, 2004.
40. Shariyat M. Thermal buckling analysis of rectangular composite plates with temperature-dependent properties based on a layerwise theory. *Thin-Walled Struct* 2007; 45: 439–452.
41. Bardella L and Genna F. On the elastic behavior of syntactic foams. *Int J Solids Struct* 2001; 38: 7235–7260.
42. Thomson WT, Dahleh MD and Padmanabhan C. *Theory of vibrations with applications*, 5th ed. India: Pearson Education, 2008.
43. Shams A and Porfiri M. A generalized Vlasov-Jones foundation model for micromechanics studies of syntactic foams. *Compos Struct* 2013; 103: 168–178.
44. Waddar S, Jeyaraj P and Doddamani M. Estimation of buckling load of fly ash cenosphere/epoxy syntactic foam composite beam through vibration tests. *J Reinf Plast Compos* 2017; ▮▮: ▮▮–▮▮.
45. Rajesh M. *Dynamic mechanical characterization of woven natural fiber polymer composite*. India: National Institute of Technology, 2017.